

XAFS and neutron diffraction study of the $\text{La}_{1-x}\text{Sr}_x\text{CoO}_3$

V. Efimov^{*1}, E. Efimova¹, D. Karpinsky², D. I. Kochubey³, V. Kriventsov³, A. Kuzmin⁴, S. Molodtsov⁵, V. Sikolenko^{1,6}, S. Tiutiunnikov¹, I. O. Troyanchuk², A. N. Shmakov³, and D. Vyalikh⁵

¹ Joint Institute for Nuclear Research, Joliot-Curie 6, Dubna 141980, Moscow region, Russia

² Institute of Solid State and Semiconductor Physics, 220072 Minsk, Belarus

³ Borekov Institute of Catalysis, Lavrentiev prosp. 5, Novosibirsk 630090, Russia

⁴ Institute of Solid State Physics, Kengaraga str. 8, 1063 Riga, Latvia

⁵ Institut für Kristallographie und Festkörperphysik (IKFP), Zellescher Weg 16, Physikgebäude C 115, 01069 Dresden, Germany

⁶ Hahn-Meitner-Institut, Glienicke Str. 100, 14109 Berlin, Germany

Received 26 July 2006, revised 30 August 2006, accepted 2 October 2006

Published online 9 March 2007

PACS 61.10.Ht, 61.12.Ld, 71.70.Ej, 75.25.+z, 75.30.Et, 76.30.Kg

We have studied the effects of hole doping on the crystal and electronic structure of the $\text{La}_{1-x}\text{Sr}_x\text{CoO}_3$ ($x = 0.0 \div 0.5$) by neutron Rietveld analysis and its correlation with the X-ray-absorption spectroscopy data. The abrupt decrease of the Co–O distance and an increase of the Co–O–Co angle upon substitution of La^{3+} by Sr^{2+} in $\text{La}_{1-x}\text{Sr}_x\text{CoO}_3$ are attributed to a change in the band structure at the transition from semi-conducting to metallic state. Upon strontium doping, a variation of Co $L_{2,3}$ -edges in $\text{La}_{1-x}\text{Sr}_x\text{CoO}_3$ series suggests an increase of the mixed low Co^{4+} and high or intermediate Co^{3+} spin states. The possible explanation of the observed changes of the crystal and electronic structure in these cobaltites is discussed.

© 2007 WILEY-VCH Verlag GmbH & Co. KGaA, Weinheim

1 Introduction The discovery of the “colossal” magnetoresistance in the manganites with perovskite structure [1] has stimulated the research of the compounds exhibiting large magnetoresistance. The magnetic and transport properties of $\text{La}_{1-x}\text{Sr}_x\text{CoO}_3$ cobaltites with perovskite structure and manganites such as $\text{La}_{1-x}\text{Sr}_x\text{MnO}_3$ have common features [2]. In both systems the substitution of La^{3+} with Sr^{2+} creates paramagnetic ($x < 0.15$) to ferromagnetic ($x > 0.3$) transition as the dopant concentration increases. The Sr^{2+} ionic radius is significantly larger than that of the La^{3+} ion, so it is possible to expect stabilization of the intermediate spin state of cobalt ions by substituting Sr^{2+} ions for La^{3+} ones. At such heterovalent substitution, Co^{4+} ions appear, leading to the ferromagnetic metallic ground state [3]. Most studies on the spin states of Co ions suggest that the trivalent and tetravalent cobalt ions remain as a mixture of low spin (LS) and high spin (HS) or intermediate spin (IS) states [4]. The majority of researchers suppose that ferromagnetism in cobaltites is caused by “a double exchange”, as in manganites [5].

In this work we present the results of neutron diffraction measurements and x-ray absorption near edge structure (XANES) study at the Co K and $L_{2,3}$ -edges of the $\text{La}_{1-x}\text{Sr}_x\text{CoO}_3$ solid solutions. The correlation between the long-range order parameters and the local electronic structure is discussed. The sensitivity of XANES to the hole-doping effects, local lattice distortion, “chemical pressure” effect and to an overlapping mixture of LS and HS or IS states of Co^{3+} and Co^{4+} ions in these cobaltites is also considered.

* Corresponding author: e-mail: klevcova@sunse.jinr.ru, Phone: +7 049621 64 173, Fax: +7 49621 65 767

2 Experimental procedure The polycrystalline $\text{La}_{1-x}\text{Sr}_x\text{CoO}_3$ samples were prepared by the ceramic method from a mixture of La_2O_3 , Co_3O_4 and SrCO_3 powders taken in stoichiometric ratios. The mixture was pressed into the pellet and heated at 1000 °C for 6 h in air. Finally, the pellet was ground, repressed, sintered at 1200 °C for 12 h in air and then cooled at a rate of 100 °C/h to room temperature.

The neutron powder diffraction experiments were carried out on the fine resolution neutron diffractometer E9 at the BER-II reactor in Hahn Meitner Institute [6]. Data were collected at 290 K over the range $4^\circ \leq 2\theta \leq 156^\circ$ with the wavelength $\lambda = 1.7973 \text{ \AA}$. The neutron powder diffraction data were analyzed with the Rietveld method using the FullProf program [7].

The Co K -edge ($E_K = 7710 \text{ eV}$) XANES spectra were recorded at the Siberian Synchrotron Radiation Center (SSRC). The storage ring VEPP-3, operated at the energy 2 GeV and an average stored current of 80 mA, was used as the radiation source.

Co 2p XAS measurements were performed on the Russian-German beamline [8] at the BESSY II in Berlin. The energy resolution of the XANES measurements at SSRC was 0.4 eV. In the Co 2p XAS measurements at BESSY II, the resolution was about 0.15 eV. All the measurements were carried out at 290 K. The XANES data analysis in the range 7690–7730 eV was performed with the program WINXAS [9]. The data were normalized by setting a point located at about 200 eV above the edge to unity.

3 Results and discussion

3.1 Neutron diffraction results Preliminary study of crystal structure of $\text{La}_{1-x}\text{Sr}_x\text{CoO}_3$ ($x = 0.0 \div 0.5$) compounds was performed using X-ray diffraction data. All observed Bragg peaks were indexed in the rhombohedral $R\bar{3}c$ space group in hexagonal axes. No impurities were present according to these data. The results of refinement of the neutron diffraction pattern are in agreement with the X-ray analysis.

The room-temperature data for $\text{La}_{1-x}\text{Sr}_x\text{CoO}_3$ ($x = 0.0 \div 0.5$) were analyzed by the profile refinement method. The result of Rietveld refinement for the $\text{La}_{0.5}\text{Sr}_{0.5}\text{CoO}_3$ is presented in Fig. 1.

3.2 X-ray absorption results The dipole-allowed $1s \rightarrow np$ transitions at the Co K -edge (7726.0 eV) dominate the XANES spectrum shown in Fig. 2. The d orbitals of cobalt mix heavily with the oxygen $2p$ orbitals [10] and the cobalt t_{2g} and e_g orbitals are expected to split by the crystal field and by the interatomic exchange energy (Hund's rule coupling) [11]. Although the $1s \rightarrow t_{2g}$ and $1s \rightarrow e_g$ transitions are forbidden in the dipole approximation, they could be experimentally observed because of oxygen p state admixing and quadrupole transitions [12]. Therefore, we attribute the pre-edge peak, appearing in Fig. 2 below 7715 eV, to the $1s \rightarrow 3d$ transition, whose energy position can be used to evaluate the valence state of cobalt. The existence of the e_g level shows Co^{3+} ion in the high or intermediate spin state. The intra-atomic exchange energy could result in additional unresolved splitting of the t_{2g} and e_g bands, thus contributing to the observed peak broadening (Fig. 2). Note that this interatomic exchange splitting could actually be comparable with the crystal field splitting [13]. An additional minor splitting is also expected from the Jahn–Teller distortions.

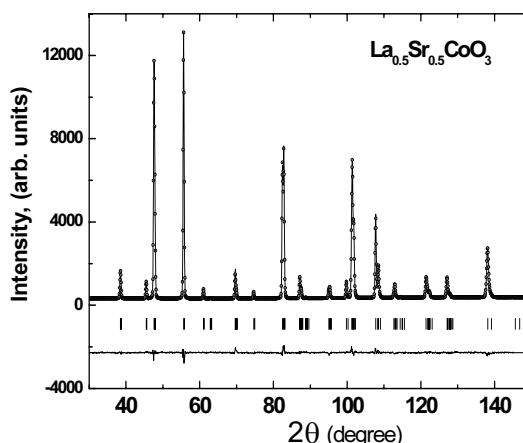


Fig. 1 Neutron diffraction pattern of $\text{La}_{0.5}\text{Sr}_{0.5}\text{CoO}_3$: experimental curve (continuous line), refinement points (open circles) and their difference (continuous line below). Ticks show the predicted 2θ positions for the Bragg peaks.

Substitution of La^{3+} for Sr^{2+} in $\text{La}_{1-x}\text{Sr}_x\text{CoO}_3$ leads to the small but observable edge shift of about 1 eV for both the t_{2g} and e_g bands to the lower energies (see Fig. 2 inset). We believe that this effect is related with the substitution of high spin Co^{3+} by the Co^{4+} ions in the low spin state.

Now we consider the correlation dependences of the Co–O–Co angle (Fig. 3) and the Co–O distance (Fig. 4), obtained from the treatment of the neutron diffraction patterns, with the intensity ratio value of the e_g and t_{2g} peaks, estimated from the analysis of XANES spectra as in [14]. It is necessary to stress that the intensity ratio of the e_g and t_{2g} peaks for LaCoO_3 is approximately equal to one (see Fig. 3 and 4).

Figure 4 shows good agreement in the behavior of the Co–O distance and the intensity ratio of the e_g and t_{2g} peaks as a function of Sr content. It should be emphasized that in the case of the Co–O–Co angle we observe a gradual increase in the deviation of the e_g and t_{2g} peaks intensity ratio while Sr content decreasing.

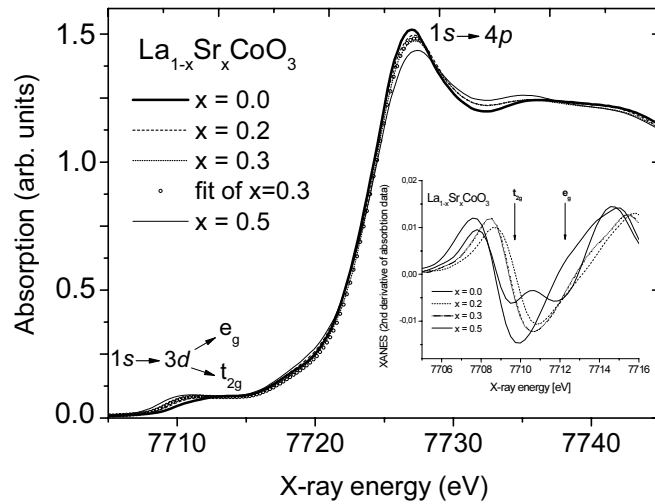


Fig. 2 Experimental Co K -edge XANES spectra for $\text{La}_{1-x}\text{Sr}_x\text{CoO}_3$ ($x = 0.0 \div 0.5$). The plot in the inset shows the 2nd derivative of the Co K -edge XANES spectra for $\text{La}_{1-x}\text{Sr}_x\text{CoO}_3$.

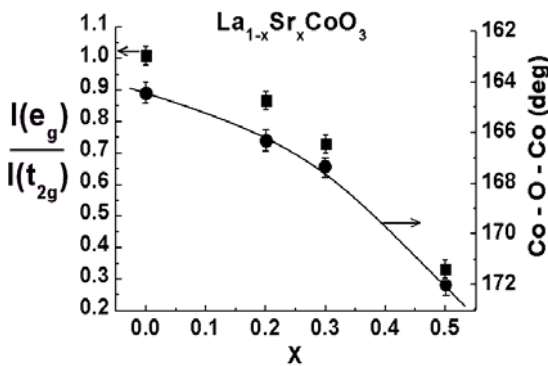


Fig. 3 The composition dependences of the Co–O–Co angle and the intensity ratio of the e_g and t_{2g} peaks of the $\text{La}_{1-x}\text{Sr}_x\text{CoO}_3$ ($x = 0.0 \div 0.5$).

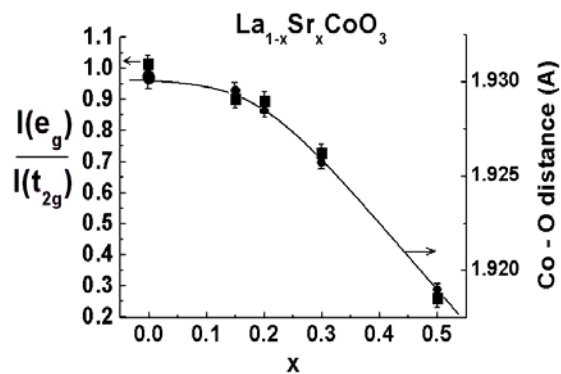


Fig. 4 The composition dependences of the Co–O distance and the intensity ratio of the e_g and t_{2g} peaks of the $\text{La}_{1-x}\text{Sr}_x\text{CoO}_3$ ($x = 0.0 \div 0.5$).

The composition dependence of the Co $L_{2,3}$ -edges XAS recorded at room temperature for the series $\text{La}_{1-x}\text{Sr}_x\text{CoO}_3$ ($x = 0.0 \div 0.5$) is presented in Fig. 5. The spectra correspond to transitions to unoccupied Co $3d$ states mixed with O $2p$ states. They are characteristic of hole-doped transition metal oxides and show the charge-transfer behaviour of the Co–O bond in the series $\text{La}_{1-x}\text{Sr}_x\text{CoO}_3$ system. Upon Sr doping, the Co- $L_{2,3}$ edges XAS peaks (Fig. 5) shift toward high energy about 0.48 eV, whereas an essential modification of the shoulder in the shape and intensity at the Co- L_3 edge is observed (Fig. 5, inset). Both indicate that new electronic states below the Fermi level are involved. They are probably due to the Co($3d$)–O($2p$) hybridization change expected upon doping and an increase of the mixed intermediate or high Co^{3+} and low Co^{4+} spin states. This result is similar to that observed in XANES measurements at the Co K -edge.

It should be emphasized that the behavior of the spectra and especially the split change value of the shoulder at the Co L_3 -edge upon the Sr doping correlates well with the behavior of the pre-edge peaks intensity ratio of the e_g and t_{2g} peaks at the Co K -edge.

On the base above considered experimental data we may conclude that gradual increasing of the difference between the intensity ratio value of the e_g and t_{2g} peaks and the Co–O–Co angle value at the gradual decreasing of the Sr content is more likely to be related with the appearance of the Jahn-Teller effect [15] that results in additional distortion of the lattice.

Acknowledgements This work was supported by Russian Fund for Basic Research (Grant N 06-02-81038).

References

- [1] P.M. Raccah and J.B. Goodenough, Phys. Rev. **155**, 932 (1967).
- [2] G. Briceno et al., Science **270**, 273 (1995).
- [3] Itoh et al., J. Phys. Soc. Jpn. **63**, 1486 (1994).
- [4] D. Louca, J.L. Sarrao, J.D. Thompson, and H. Roder, Phys. Rev. **60**, 10378 (1999).
- [5] C. Zener, Phys. Rev. **81**(3), 440 (1951).
- [6] D. Tobbens, N. Stußer, K. Knorr, and G. Lampert, Mater. Sci. Forum **378–381**, 288 (2001).
- [7] J.L. Rodríguez-Carvajal, Physica B **55**, 192 (1992).
- [8] S.I. Fedoseenko, D.V. Vyalikh, S.L. Molodtsov et al., Nucl. Instrum. Methods Phys. Res. A **505**, 718 (2003).
- [9] T. Ressler, J. Synchrotron Radiat. **5**, 118 (1998).
- [10] D. Koningsberger and R. Prins, X-ray Absorption, Principles, Applications, Techniques of EXAFS, SEXAFS and XANES (Wiley, New York, 1988), p. 11.
- [11] C. Zobel, M. Kriener et al., Phys. Rev. B **66**, 020402 (2002).
- [12] A. Bianconi et al., Phys. Rev. B **26**, 2741 (1982).
- [13] O. Toulemonde, N. N'Guyen, and F. Studer, J. Solid State Chem. **158**, 208 (2001).
- [14] O. Haas, R.P.W.J. Struis, and J.M. McBreen, J. Solid State Chem. **177**, 1000 (2004).
- [15] J. Bala and A. M. Oles', Phys. Rev. B **62**, 6085 (2000).

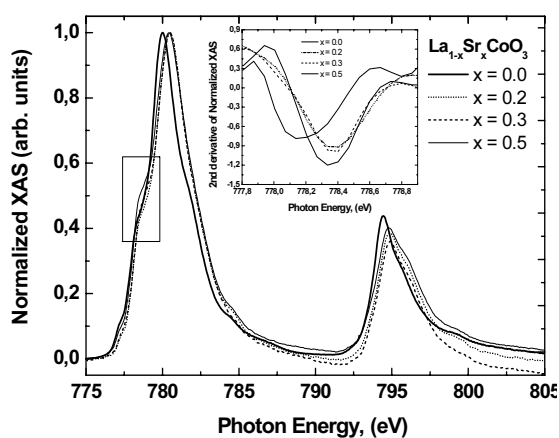


Fig. 5 Normalized XAS at the Co $L_{2,3}$ -edges of $\text{La}_{1-x}\text{Sr}_x\text{CoO}_3$; the plot in the inset shows second derivative of normalized XAS at the Co L_3 -edge shoulder.